CHAPTER III

REVIEW OF THEORETICAL BACKGROUND AND LITERATURES

3.1 Cellulose, Bacterial Cellulose, Bacterial Cellulose based Nanocomposite

3.1.1 Cellulose

Cellulose, the most common bio-polymer, has been used for centuries as a raw material from trees and other plants in various applications. However, it was first isolated from plant matter by French chemist Anselme Payen in 1839. He reported that cellulose has an identical structure as starch, but it exhibited the difference in structure and properties. Up to now, cellulose is commonly known as a polysaccharide with the common formula $(C_6H_{10}O_5)_n$, and consisting of a linear chain of several hundreds to over thousand linked glucose units.

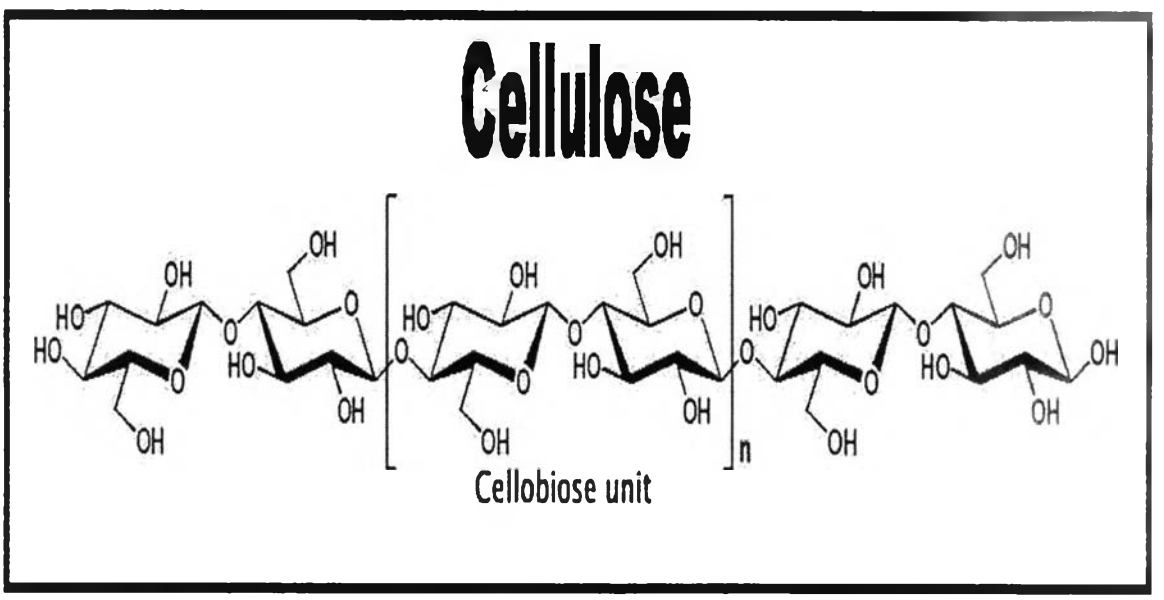

Figure 3.1 Chemical structure of cellulose

Figure 3.1 exhibits the chemical structure of cellulose. Cellulose composes of several glucose units in order to form long linear chain, so-called "polysaccharide". In general, it is commonly known that cellulose can be produced from plants or bacterial. Cellulose is exacted from plant material such as wood, flax, hemp, sisal or

cotton. For plants, cellulose is found in a composite form composed of polymers, lignin and carbohydrates as hemicelluloses and cellulose which are physically and chemically bound together [26]. The matrix which is lignin in plants matter bonds the cellulose fibers together acting as resin system. Cellulose and hemicellulose act as reinforcement material and interfacial compatibilizer between cellulose and lignin, respectively. Although cellulose constitutes a significant portion of material, mechanical properties such as tensile strength and stiffness of the plain material are inferior to the properties of neat cellulose. When comparing to natural fibers, it can be observed that mechanical properties such as tensile strength and Young's modulus commonly drop with lower cellulose content [27]. For high strength materials, it would clearly be preferable to contain as much cellulose in a natural material as possible.

Table 3.1 Composition and comparative properties of natural and man-made fibers [27].

Types of Fibre	Cellulose (%)	Lignin (%)	Hemi-cellulose (%)	Pectin (%)	Wax (%)	Tensile strength (MPa)	Young's modulus (GPa)
Fruit							
Coir	36-43	41-45	0.15-0.25	3-4	-	131-175	4-6
Bast							
Jute	61-71.5	12-13	13.6-20.4	0.2	0.5	393-773	13-26.5
Flax	71	2.2	18.6-20.6	2.3	1.7	345-1100	27.6
Hemp	70.2-74.4	3.7-5.7	17.9-22.4	0.9	0.8	690	-
Ramie	68.6-76.2	0.6-0.7	13.1-16.7	1.9	0.3	400-938	61.4-128
Leaf							
Sisal	67-78	8.0-11.0	10.0-14.2	10.0	2.0	468-640	9.4-22.0
PALF	70-82	5-12	-	-	-	413-1627	34.5-82.51
Seed							
Cotton	82.7	-	5.7	-	0.6	287-800	5.5-12.6
Man-Made							
E-glass	-	-	-	-	-	2000-3500	70
S-glass	-	-	-	-	-	4570	86
Aramid	-	-	-	-	-	3000-3150	63-67
Carbon	-	-	-	-	-	4000	230-240

Apart from natural plants, there are however some different species of bacteria that can produce pure cellulose. Certain bacteria belonging to the genera Acetobacter, Agrobacterium, Alcaligenes, Pseudomonas, Rhizobium or Sarcina were

reported capable of producing cellulose, the most efficient producer being Acetobacter xylinum [28]. Bacterial cellulose is chemically the same as plant cellulose, which is β-1,4-glucans. In the next sub-chapter the bacteria cellulose will be described in detail.

3.1.2 Bacteria Cellulose

Bacterial cellulose (BC) was first written about in a scientific paper by Brown in 1886 [15]. It is chemically the same as plant cellulose, which is β-1,4-glucans (Figure 2.1). The papers described a fermentative process which formed a gelatinous transparent membrane at the surface of an acetic fermentation. The membrane had the capability to grow to a thickness of 25 mm and proved to be very strong and tough. It also called pellicle, proved to be cellulose formed by a bacterium. The bacterium was named Bacterium Xylinum by Brown, but later it was classified as Acetobacter Xylinum. However, in general, Certain bacteria belonging to the genera *Acetobacter*, *Agrobacterium*, *Alcaligenes*, *Pseudomonas*, *Rhizobium* or *Sarcina* were reported capable of producing bacterial cellulose, the most efficient producer being *Acetobacter xylinum* [29]. In Table 3.2, it exhibits a classification of bacteria's capability to produce cellulose.

Table 3.2 A classification of the bacteria's capability to produce cellulose [30]

Genus	Cellulose structure
Acetobacter	*pellicle composed of ribbons*
Achromobacter	*fibrils*
Aerobacter	*fibrils*
Agrobacterium	*short fibrils*
Alcaligenes	*fibrils*
Pseudomonas	*no distinct fibrils*
Rhizobium	*short fibrils*
Sarcina	*amorphous cellulose*
Zoogloea	*not well defined*

Acetobacter xylinum is a strain of acetic acid-producing bacteria and an obligate aerobe. Cellulose is a hydrophilic glucan polymer which contains hydroxyl groups. These hydroxyl groups can form intramolecular hydrogen bonds inside the macromolecule itself and among other cellulose macromolecules as well as with hydroxyl groups from the environment [31]. In the bacterial culture, the bacterial cellulose microfibrils agglomerate and form a pellicle, which will provide a firm matrix that floats and, therefore, allows the embedded bacteria to stay in close contact with the atmosphere. The produced cellulose pellicles play an important role in promoting colonisation of the cells on the substrate and provide protection against competitors. Cellulose pellicles were also observed to protect *Acetobacter xylinum* cells from UV light [32].

Bacterial cellulose has been substantially utilised in food industry [33]. An example is nata de coco, a coconut gel dessert prepared by bacterial fermentation of coconut water. Though originally the Filipino dessert, it becomes very popular as diet food in Japan [15, 29]. Also, owing to its good liquid adsorption, ability to withstand sterilisation and non-allergenic properties, bacterial cellulose is extensively employed in many medical applications. The examples are artificial skin, blood vessels and ureters [29, 34]. Bacterial cellulose is also applied as a binder in the paper industry to improve the strength as well as the durability of paper. Other uses includes diaphragms in audio components [29, 33]. The growth of *Acetobacter xylinum* and its production of bacterial cellulose are governed by its carbon source, nitrogen source and the condition of the culture system. Many carbon sources were studied as reported in the literature [35]. Romano et al. [15] studied the effect of carbon source on the production of bacterial cellulose. It was found that galactose and xylose gave lower yields than glucose due to slower growth rates of the bacteria. Masaoka et al. [36] reported that the bacterial cellulose yield from sucrose was only half the yield from glucose whilst fructose and glycerol gave almost the same cellulose yield as glucose. The sugar alcohol, arabitol [37] and mannitol [38], were reported to yield 6.2 and 3.8 times more cellulose than glucose. It was shown that these sugar alcohols were matabolised via xylulose and fructose and that no gluconic acid was produced during fermentation, which consequently resulted in more stable pH of the culture. Other carbon sources, such as 5- or 6-carbon monosaccharides,

oligossaccharides, starch, alcohol and organic acid were also reported [39] as well as the methylated glucose derivative [40].

Acetobacter xylinum also requires a specific complex nitrogen source such as yeast extract and peptone for its growth [29]. Amino acids such as methionine and glutamate are claimed to have an important effect on the cell growth and the cellulose production [41-43], while the pyridoxine, nicotinic acid, p-aminobenzoic acid and biotin are the most stimulating vitamins [41, 44]. However Fielder et al. [45] did not observe any positive effect on cellulose synthesis of vitamins. Some other compounds that can strongly stimulate cellulose production includes derivatives of choline, betaine and fatty acids [46]. Corn steep liquor, which is a viscous concentrate of corn solubles that is rich in vitamins, amino acids, minerals and other growth stimulants, is also found to be suitable for cellulose production by *Acetobacter xylinum* strain *Gluconacetobacter xylinus* BPR 2001 [47]. It was reported that when lactate, which was detected in corn steep liquor, was added to culture media containing other nitrogen sources, the bacterial cellulose production was enhanced to the level similar to those in the medium containing corn steep liquor [44]. In terms of the bacterial culture system, studies indicate that the optimal pH range for the production of bacterial cellulose by *Acetobacter xylinum* is in the range of 4–6 [44] while the optimal growth temperature is in the range of 25–30 °C [23]. Variation in temperature can cause changes to the degree of polymerisation of the cellulose and its water-binding capacity [29]. Oxygen transfer is particularly crucial to bacterial cellulose production. It has been found that when oxygen-enriched air was supplied into the system, the concentration of bacterial cellulose was two times higher than that of air-supplied culture and comparable to that in a mechanically agitated stirred-tank fermentor, but with much lower energy consumption. The size of the cellulose pellets also strongly depends on the amount of dissolved oxygen in the broth [48]. Bacterial cellulose formed under a low oxygen environment has relatively fewer ramifications comparing to those formed under a higher oxygen environment [42]. However, high levels of operating pressure (oxygen and other gas pressures) have been reported to inhibit the bacterial growth [29].

The conventional method for the production of bacterial cellulose is static cultivation using sugars such as glucose, fructose and sucrose. However, this method is not applicable to large-scale industrial production due to the long cultivation time and expensive carbon source [49]. Other culture systems have been investigated; rotating drum fermentors were reported by Fiedler et al. [50] and Sattler and Fiedler [51], and was reported to give higher yields than static systems. However, it was later shown [35] that it is difficult to obtain good quality pellicles and that the rotating system is not successful enough for more intensive studies for industrial purposes. Bacterial cellulose production in stirred-tank reactors and aerated reactors has also been reported [28, 48, 52, 53]. In terms of the cellulose quality, the bacterial cellulose cultured in static system exhibits a more compact and denser structure than those cultured in agitated systems. It also has much higher degree of polymerisation, crystallinity index and Young's modulus [54] (Table 3.3). In addition, the agitated systems were reported to offer lower productivity than the static system due to its spontaneous generation of cellulose-negative mutants which do not produce cellulose [55, 56]. Czaja et al. [15] reported that mostly uniaxially oriented ribbons cellulose was formed in the static culture, whereas cellulose synthesised under agitating condition demonstrated a structure of disorderly, curved and overlapping ribbons. Such a disordered microstructure could result from constant shear forces during the agitation [47, 57].

Formation of bacterial cellulose

The synthesis of cellulose in *Acetobacter xylinum* occurs between the outer cell membrane and cytoplasma membrane by a cellulose-synthesising complex [15, 23, 58] which is associated with pores at the surface of the bacteria (Figure 3.3) [32, 59]. The cellulose synthase [15, 23, 32] is considered to be the most important enzyme in this process. The cellulose produced leaves the pores as fibrils and joins together with many other fibrils to form a ribbon of crystalline cellulose. The ribbon elongates in direct association with the cell envelope and remains associated during cell division [15, 60, 61]. The self-assembly process should be responsible for the crystallisation of the obtained cellulose [32].

Some authors [23, 45] suggested that the process of cellulose formation should occur at the medium/pellicle interface and that the producing bacteria should be near this interface. Borzani and Souza [62] demonstrated that the real site for the cellulose formation was at the upper side of the pellicle at the air/pellicle interface, which meant that the producing cells as well as nutrition must to be transported through the pellicle to its surface.

A principal biochemical pathway from glucose to cellulose is shown in Figure 3.4. [23, 32]. A single *Acetobacter xylinum* was reported of being capable of polymerising up to 200,000 glucose molecules per second into a cellulose chain [39]. Apart from the cellulose, other by-products are also synthesised such as carbon dioxide, acetan, which is a branched polymer of β-1,4-glucose, acetic acid, and gluconic acid. The synthesis pathway of bacterial cellulose by *Acetobacter xylinum* was explained in greater detail by Ross et al. [32].

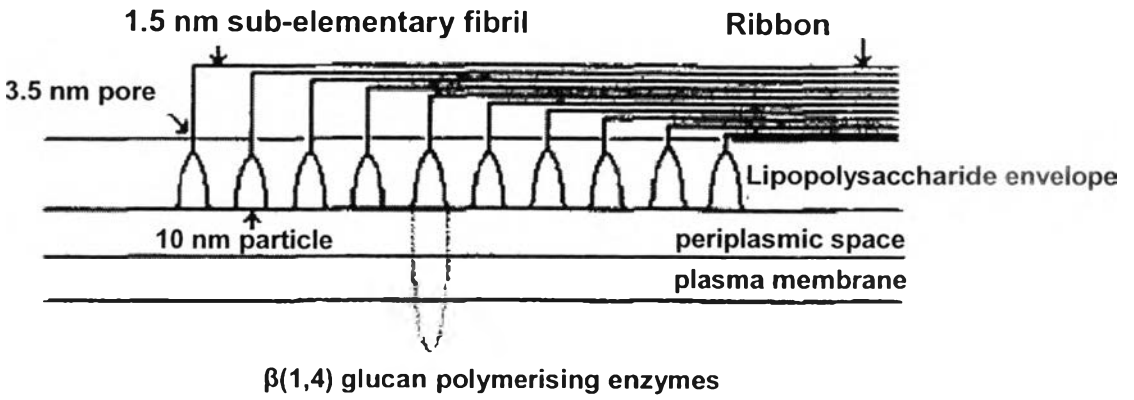

Figure 3.2 Scheme for the formation of bacterial cellulose. Reproduced from Jonas and Farah [35].

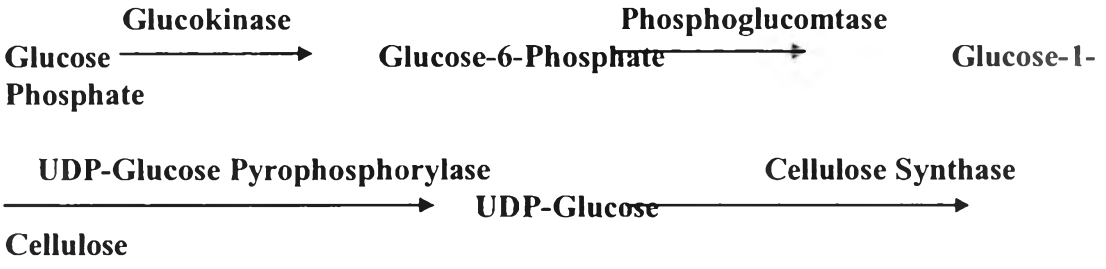

Figure 3.3 Proposed biochemical pathway for cellulose synthesis in *Acetobacter xylinum*. Reproduced from Cannon and Anderson [23].

Properties of bacterial cellulose

Bacterial cellulose synthesised by *Acetobacter xylinum* has been extensively investigated by Czaja et al. [15] (strain NQ-5) and Watanabe et al. [16] (strain BPR2001). Some of the reported properties are listed in Table 3.1. An air-dried bacterial cellulose sheet has tensile strength of 256 MPa with the Young's modulus of 17 GPa [63]. The elastic modulus of bacterial cellulose single fibril was recently measured using atomic force microscopy (AFM) by Guhados et al. [64] to be 78 GPa, which is comparable to glass fibre. The elastic modulus of the bacterial cellulose single fibril was also estimated using a Raman spectroscopic technique to be 114 GPa by Hsieh et al [14]. This modulus was predicted from a calibration of the Raman band shift against the elastic modulus. In comparison, the elastic modulus of the crystalline cellulose (Cellulose-I) was measured by X-ray Diffraction (XRD) to be 138 GPa as reported by Nishino et al. [65].

Table 3.3 Properties of bacterial cellulose.

Features	Watanabe et al. [16]		Czaja et al. [15]	
	Agitated Culture	Static Culture	Agitated Culture	Static Culture
Crystallinity index (%)	63	71	-	-
Crystallite size (nm)	6.9	7.4	6.4-7.9	6.7-8.6
Crystallinity (%)	72	80	84	89
Cellullose Iα (%)	61	73	71	76
Degree of polymerisation	10900	14400	-	-

Advantages of Bacterial cellulose for use as composite materials

The main advantage of bacterial cellulose is its biodegradability and environmentally friendly aspect. In the last few years, various technological innovations have been pressed by the world's concern with the depletion of natural resources and the impact of technology on the environment and climate change. Ultimately, there is a strong focus on renewable and biodegradable materials [27]. An important issue with most natural materials used nowadays refers to the mechanical properties with are far more inferior to the properties of synthetic materials such as glass, carbon fiber and aramid used in various different applications, due to their high performance and versatility. Bacterial cellulose is one of innovative materials capable to incorporate the renewability and biodegradability of natural materials with high mechanical properties of glass fibers. Figure 3.4 shows the renewability and Biodegradability cycle of bacterial cellulose.

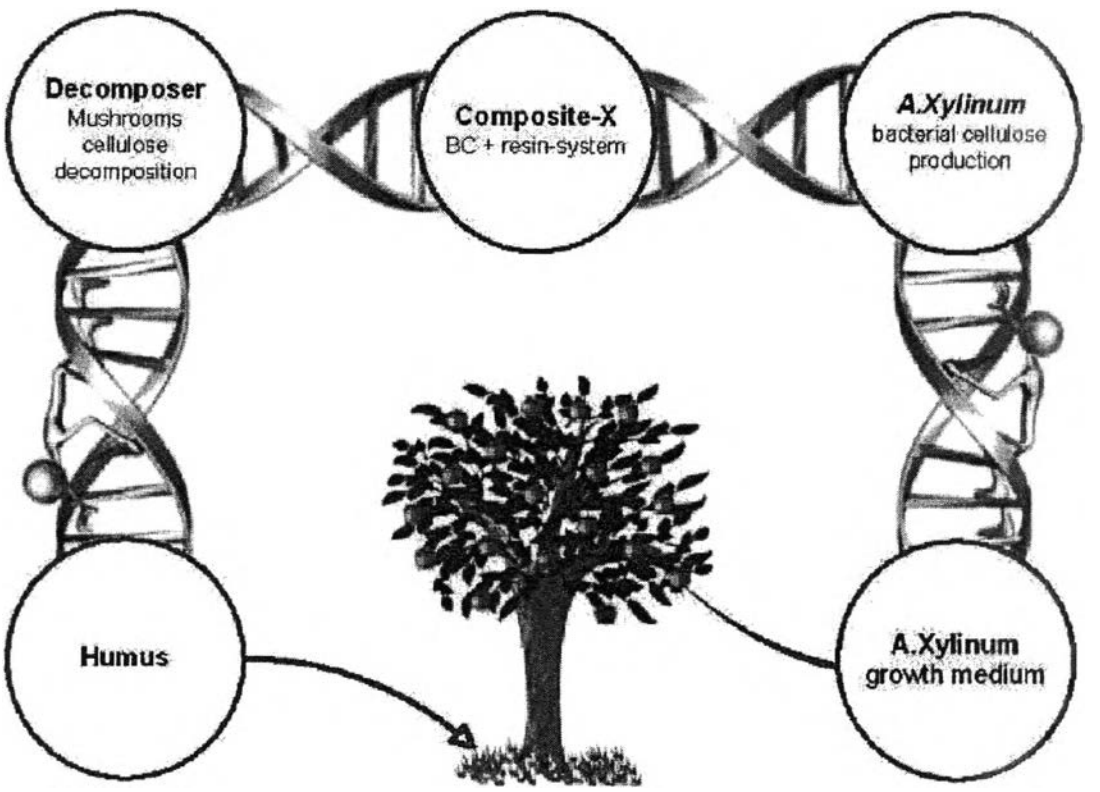

Figure 3.4 Renewability and Biodegradability cycle of bacterial cellulose

According to many literatures, bacterial cellulose has been used as raw material for composite industries having the following mechanical characteristics:

- In 2004, Gindl et al [33] reported the result of a set of tensile tests performed on cellulose acetate butyrate reinforced with bacterial cellulose. They fabricated the composite by solvent evaporation casting. The composite material composed of 10-30% volume of cellulose and exhibited the Young's modulus as 3.2-5.8 GPa and a tensile strength 52.6-128.9 MPa. Moreover, they reported an increase in the elastic modulus that occurred while the specimens were cyclic tensile loaded and unloaded

- In 2005, The Research Institute for Sustainable Humanosphere, Kyoto University, Japan published the relevant papers regarding the production of a hybrid bacterial cellulose composite [11]. They reported the processing of bacterial cellulose sheets was impregnated with phenol-formadehyde resin in order to form a laminar composite. The composites were subjected to a three-point bending test and tensile test. They concluded that Young's modulus for the bacterial cellulose based composite is 28 GPa and the tensile strength up to 420 MPa. The higher modulus of bacterial cellulose composites was credited to the fine and uniform 3D structure formed by A. Xylinum. The high performance of mechanical properties is directly connected with the bi-dimensionally orientation of the uniform nanoscale network formed by A. Xylinum.

Other advantages of bacterial cellulose refer to processing step: the wear on milling tools is almost negligible compared to that on tools used for the fabrication of parts of metal or synthetic composite parts. Comparison to glass, it has lower density and favorable energy absorption, good acoustic and thermal properties. It offers higher toughness than glass, which means it does not splinter like glass fiber. It has the potential for one-step manufacturing even of complex construction elements and it has the capability to be made almost completely transparent. Health risks that come with splintering of the material or use of toxic materials are much smaller when working with bacterial cellulose. In addition, production of metals, glass and carbon fibers requires very high production temperatures as well as a lot of energy, which also dominated the price.

One of the most attractive characteristics of bacterial cellulose for researchers is the fact that bacterial cellulose can be produced in predetermined shapes. Because bacterial cellulose is formed on the interface between air and culture medium, the shape of the cellulose is directly determined by the shape of the interface medium.

3.1.3 Bacterial Cellulose Reinforced Composites

Bacterial cellulose reinforced composite materials consist of bacterial cellulose of high strength and modulus embedded in or bonded to a matrix with distinct interfaces (boundary) between them. In this form, both bacterial cellulose and matrix retain their physical and chemical identities, yet they produce a combination of properties that cannot be achieved with either of the constituents acting alone. In general, bacterial celluloses are the principal load-carrying constituent while the surrounding matrix keeps the bacterial celluloses in the desired location and orientation, and acts as a load transfer medium between them. The matrix also protects the reinforcing bacterial celluloses from environmental attack due to temperature and humidity, for example. Thus although the bacterial celluloses provide reinforcement for the matrix, the matrix also serves a number of useful functions in composite materials [66]. The mechanism of reinforcement can be explained as the transfer of the stress applied to the composite to the reinforcing bacterial celluloses by the deformation of the matrix material around the bacterial celluloses. Assuming that a good bond is maintained between the bacterial celluloses and the matrix, when stress is applied to the composite, the bacterial celluloses will resist strain locally and a much higher stress will be induced in the bacterial celluloses than in the matrix around them. The matrix around the bacterial celluloses will be constrained and will suffer shear at the area near the bacterial cellulose tips. This shear of the matrix is the dominant process in determining the composites properties [67]. To illustrate this fact it is only necessary to imagine a deformable sheet on which two sets of equally spaced lines are drawn perpendicular to one another. This construction gives a regular pattern of identical squares. If the sheet is uniformly stretched in the direction of one of the sets of lines, the squares become rectangles, retaining the 90° angle in each corner of the original squares. However if a bacterial cellulose is embedded into the original undeformed sheet (matrix), as the

sheet is stretched, the results can be illustrated in Figure 5. Part of the sheet that is adjacent to the bacterial cellulose is obliged to follow the deformation of the stiffer bacterial cellulose whilst further away the sheet can deform to a larger extent. The result is that there are no longer intersections of the lines at right angles. The effect will be greatest in the neighbourhood of the bacterial cellulose tips. The presence of the bacterial cellulose has caused a stress concentration in the area near the two bacterial cellulose tips and much lower stress around the body of the bacterial cellulose. However this stress concentration at the tips can be reduced if the stress can be transferred to the adjacent bacterial cellulose. Therefore, reinforcing bacterial celluloses must be close enough to one another in order to maximise the reinforcing effect, which can be achieved by an acceptable dispersion level of bacterial celluloses into the matrix [67, 68].

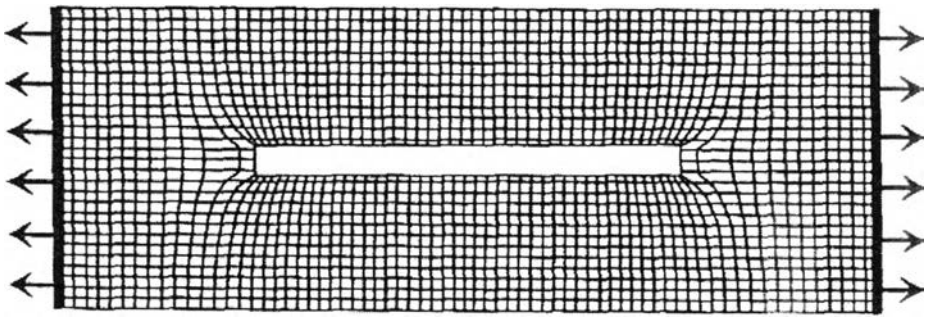

Figure 3.5 Deformable sheet with embedded bacterial cellulose: the lines show deformation of the sheet when stretched. Reproduced from Bunsell and Renard [67].

The properties of composites are strongly influenced by the proportions and properties of the matrix and the reinforcement. Most properties of a composite are a function of a number of parameters as the constituents usually interact in a synergistic way. The strength of the interface between the bacterial cellulose and the matrix is particularly important in determining the properties of the composites. The interfacial bond strength has to be sufficient for load to be transferred from the matrix to the bacterial celluloses if the composite is to be stronger than the unreinforced matrix. Other parameters which may significantly affect the properties

of a composite are the shape, size, orientation and distribution of the reinforcement within the matrix as well as various features of the matrix such as the crystallinity and the grain size for crystalline polymer matrix [69].

Structural properties of porous bodies in composite

Generally, bacterial cellulose composite has high water absorption behavior. This characteristic must be considered because it will interrupt and decrease the performance of bacterial cellulose composite. In general, water absorption can be determined by two methods: the one – the bacterial cellulose composite has porous structure, the other one – the bacterial cellulose can form hydrogen bonding with water. It is commonly known that cellulose is insoluble in water; it can form hydrogen bonds with water. To a certain extent, any materials can have porous structure and absorb water. From a fundamental point of view of this phenomenon, the structural properties of porous bodies are described below.

A porous environment is considered to be solid containing pores. A geometrical definition of pore concept is hardly to determine. Generally, pores are considered hollow spaces distributed inside the solid that can connect or not between each other, being close or open between faces. The connecting portion of pore is commonly referred to as effective pore space or simply effective porosity. This definition is largely used in filtering technology where porous bodies can have a high total porosity related to a low effective porosity. Total porosity is always superior to the effective one [30]. In general, porosity is defined as the ratio between pore's volume and form volume:

$$\Phi = V_{pore} / V_{f}$$

Along with volume porosity, there is the concept of surface porosity, defined as the ratio between the pore's ending area existing onto a sectioned surface of the porous form and the area of the sectioned surface

The simplest model of the porous body is a system of short radius and equal-form particles (monodisperse system). Any polydisperse system can be fragmented into monodisperse system by real or hypothetical metric analysis.

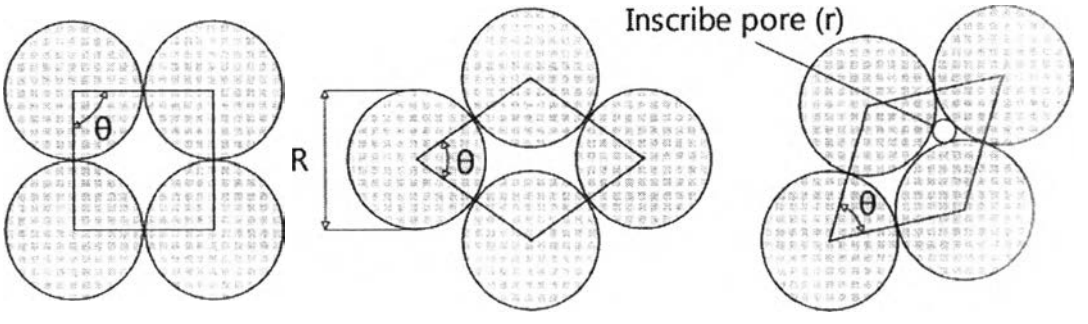

Figure 3.6 Solid particles layout in forming a cell inside the porous layer

Figure 3.6 exhibits the spherical particles can be arranged in different ways. The limits are a rare layout (a, cubic) and a dense layout (c, hexagonal). Between these limits there are all real layouts. In the ideal case, if the particles do not form hydrogen bonds with water, water holding capacity will be directly proportional with the porosity volume.

On the other hand, the mechanical properties of composites are generally described below where the pore's volume can be substituted by the matrix volume.

$$P_c = (P_f V_f) / (P_m V_m)$$

Where:

P_c – Mechanical properties of composite

P_f – Mechanical properties of fiber

V_f – Volume fraction of fiber

P_m – Mechanical properties of matrix

V_m – Volume fraction of matrix

A fundamental parameter of the composite's micromechanics is the representative volume element, for a composite with unidirectional fibers, is sketched in Figure 3.7.

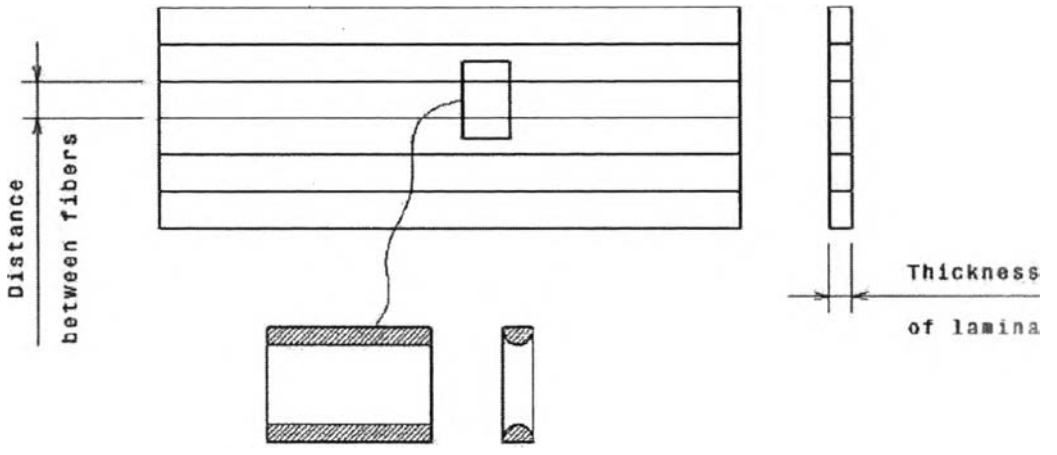

Figure 3.7 Representative volume elements in composite

This volume element represents the smallest portion within composite material, where stresses and strains are considered to be macroscopically uniform. Microscopically, these stresses and strains are non-uniform because composite material is not homogeneous. For a 3D orientation of the bacterial cellulose, the microscopic representation is more complicate. For simplification, it will be easier to consider two directions and exact an empirical coefficient for third direction. In this case, if the wiring geometry is neglected, then two reference dimensions of the volume element are the distances between the bacterial cellulose, one of each direction, and the third dimension is imposed by the number of bacterial cellulose layers in the direction of the material thickness.

The micromechanical analysis of a composite is based on the following simplified hypothesis:

- Lamina is considered macroscopically homogenous and orthotropic, linearly elastic and without initial internal stresses.

- Fibers are considered homogeneous and isotropic, linearly elastic, having a regular position and being perfectly aligned.

- Matrix is considered homogeneous and isotropic, linearly elastic and having a perfect adherence to the fibers.

Regarding material porosity, it is acknowledged that hollow spaces inside a porous material can be interior (closed) pores, exterior (open at both ends) pores and

inter-granular pores or unoccupied spaces. Monofilament fabrics and granular layers of non-porous particles generally have inter-granular spaces. In operations involving flows through porous structures (filtering, capillary pumping etc.), the porosity corresponding to inter-granular spaces and sometimes to open pores presents interest. Pore size distribution is also important, though pore "size" or "diameter" is a simplified notion, because pores are far from having cylindrical form. Most commonly, they have irregular forms with contractions and ramifications. This is why a porous material is preferably characterized by the notion of permeability. But there are cases, especially regarding membranes, that consider as important the size of the pores.

This theory stands just in the case when cellulose does not form hydrogen bonds with water or when mechanical properties of the material are evaluated for water free environments. However, in the next part of this chapter the *"cellulose-water relation is analyzed"*.

Cellulose hydrogen bonding and cross linking

Cellulose has no taste, is odorless, *hydrophilic*, insoluble in water and most organic solvents, chiral and it is also biodegradable. It can be broken down chemically into its glucose units by treating it with concentrated acids at high temperatures. In pure form, cellulose always absorbs water, which has a plasticizer effect upon it. It is acknowledged that fabrics of cellulosic fibers exhibit good dimensional stability in the dry state, but can shrink and/or wrinkle when wet. This occurs because, in dry state, the cellulose chains are held together by extensive networks of hydrogen bonds between the hydroxyl groups of adjacent chains in its structure. In other words, the hydrogen bonds form a cross-linked structure. If a stress, such as twisting or folding, is applied to the dry fabric, the hydrogen bond cross-links tend to hold the chains in position and cause the fabric to return to their original position when the deforming stress is removed. However, when the fabric is brought into contact with moisture, water molecules can participate in the hydrogen bonding and penetrate between the cellulose chains, effectively breaking up the

cross-linked structure. The water molecules act as a plasticizer for cellulose and the chains may move relative to each other. If the fabric becomes wrinkled in the moist state, the chains move to relieve the strain and there is no effective force to return the fabric to its original shape when the stress is removed. Thus, for cellulosic fabrics to exhibit durable press (also termed permanent press or wrinkleresistant) characteristics, it is necessary to form cross-links which are not easily broken by water. This is usually done with formaldehyde or formaldehyde derivatives, such as urea-formaldehyde resins.

Several research groups have mentioned that, in case of bacterial cellulose, one of the major problems with producing a composite out of this material is the presence of hydroxyl and other polar groups within its structure. This makes it highly hydrophilic and therefore it doesn't bond optimally with commonly used resins like epoxy or polyester as they cannot wet the fibers sufficiently. Another problem is the strong crystalline content of cellulose which inhibits the penetration of resin [27, 70].

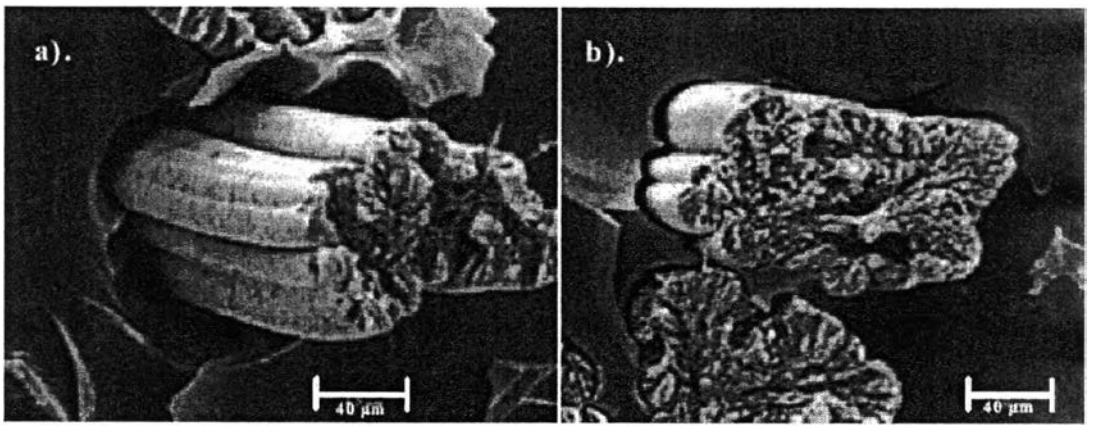

Figure 3.8 SEM of fracture surfaces of epoxy composites based on long viscous fibers (a) without treatment (b) after treatment with silane [71]

To overcome these issues, some researchers have modified the cellulose by adding hydrophobic elements to the molecular structure and thereby improving the adhesion to hydrophobic resins. Abdelmouleh [71] describes a method of treating plant cellulose with silanes that react with the OH groups of the cellulose and gives it a hydrophobic character. Composites that were made with polyester and epoxy clearly showed an improvement in bonding between the fibers and resin (Figure 3.8).

When flexural tests were performed the results revealed an increase in flexural strength of up to 40%. However, the author did not report studies on the composite's water sorption behavior. Mohanty [27] describes several methods of treating natural fibers, aiming to improve adhesion characteristics. For example, alkali treatment can remove the hydroxyl group and replaces it with a Na+ ion, which makes the surface rougher and therefore improve the mechanical interlocking of the cellulose with the resin, but also depolymerises the native cellulose. Graft copolymerization was used to graft vinyl monomers onto natural fibers that are compatible with several resin systems. Etherification was done by cyanoethylation and acetylation was used to produce esterified natural fibers which both results in plastic behavior. Isocyanate groups were used to react with the hydroxyl groups in order to form strong covalent bonds and create better compatibility with binder resins. Treatment with polypropylene is believed to increase the surface energy of the fibers and therefore further increase the wettability and interfacial adhesion.

Very good results were obtained also when cellulose was used as matrix. In 2004 Nishino et al, [65] published the Paper "All-Cellulose Composites", in which they characterize a new type of composite having cellulose as matrix and cellulose fibers as reinforcement fibers. In their studies they used refined ramie as cellulose fibers and for the matrix they used pretreated craft pulp from coniferous trees solved in 8% LiCl. The new composite revealed a tensile strength of up to 480 MPa, this strength being the highest tensile strength ever reported on any cellulose based composite. However, the author did not reported studies on the composite's water absorption capability.

Here, the detail presented above is the fundamental theory of cellulose and cellulose based nanocomposite materials. The highlight of this research of this research is to develop cellulose based nanocomposite as a flexible substrate for organic light emitting diodes (OLEDs)

3.2 Organic Light Emitting Diodes (OLEDs)

3.2.1 Basic OLEDs Structure and Materials

OLEDs are essentially several thin organic film semiconductors sandwiched between two electrodes. A schematic cross-section of an OLED with two organic layers is shown in Figure 2.9.

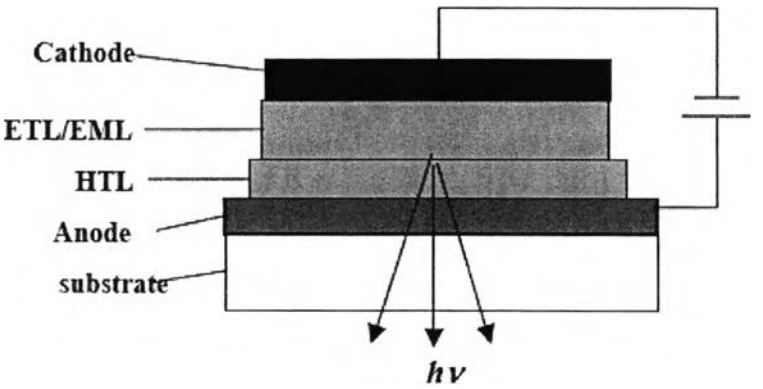

Figure 3.9 OLED structures. The total organic thin film thickness is typically ~ 100 nm.

The cathode, top electrode, consists of a low work function metal, typically Al, or Mg: Ag deposited by thermal evaporation. The anode, bottom electrode, is a thin film of the transparent semiconductor indium tin oxide (ITO) deposited onto glass substrate by sputtering. The most commonly used organic materials in OLEDs are: TPD or NPB, as a hole transport layer (HTL), and Alq as an emissive layer (EML) and electron transport layer (ETL). Their molecular structures are shown in Figure 3.10. Light is emitted through anode if the diode is operated under a sufficient forward bias.

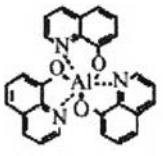

Alq

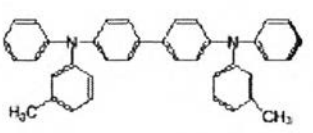

TPD

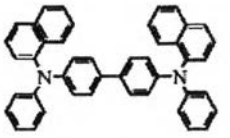

NPB

Figure 3.10 Structure of some molecular semiconductors that have been used in OLEDs. Alq is used as an electron transport and emissive layer, TPD or NPB is used as a hole transport layer.

Table 3.4 The basic properties of OLED materials

Material	Glass transition temperature (°C)	Optical gap (LUMO-HOMO) (eV)	Ionization potential (eV)	Electron mobility ($cm^2v^{-1}s^{-1}$)	Hole mobility ($cm^2v^{-1}s^{-1}$)
Alq	172 [72]	2.8 [73]	5.7 [73]	$10^{-6} - 10^{-5}$ [74]	$2*10^{-8}$ [75]
NPB	95 [76]	3.3 [77]	5.2 [73]		$8.8*10^{-4}$ [78]
TPD	63 [79]	3.1 [80]	5.4 [80]		$> 10^{-4}$ [16]

Device functionality is based on the properties of materials. The understanding of materials is of great importance to the further improvement of OLEDs. Considerable research efforts have been aimed at studying the basic properties of those molecules, especially Alq. Some well-documented data are summarized in Table 4. Basically, there are two major concerns. Low glass transition temperature of HTMs such as TPD and NPB is an issue to device reliability. The crystallization of HTM, which can occur at room temperature and can be accelerated by the Joule heat generated during device operation, is one of the important factors resulting in OLED degradation. [81] The other concern is that the electron mobility of Alq is ~ 2 orders of magnitude lower than the hole mobility of HTM. That can lead to unbalanced electron and hole current.

3.2.2 Device Operation and Efficiency

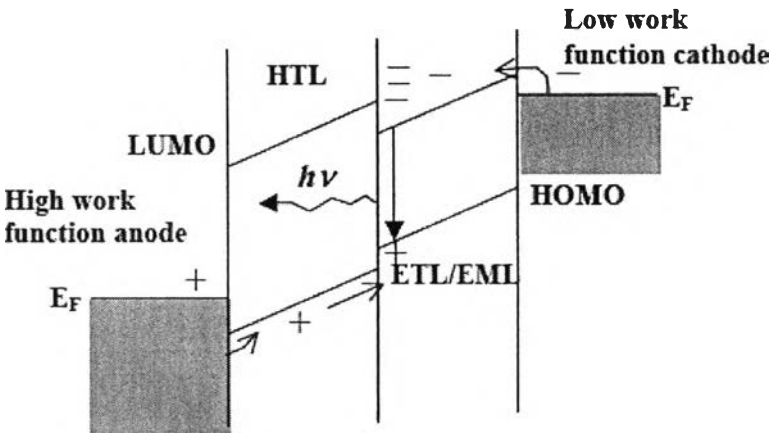

Figure 3.11 Schematic energy level diagram of OLEDs under forward bias

Figure 3.11 illustrates the energy level diagram between interfaces in OLEDs under a bias, corresponding to the OLED configuration as shown in Figure 9. Under a forward bias, holes from the anode are injected into the highest occupied molecular orbital (HOMO) of the HTL, and in the meantime, electrons are injected from the cathode into the lowest unoccupied molecular orbital (LUMO) of the ETL. The recombination of holes and electrons results in photon emission. The radiative recombination occurs at the organic/organic interface, which generally is within the ETL. The organic/electrode and organic/organic interfaces play a very important role in the performance of OLEDs. Therefore, the understanding of the mechanisms controlling the energy barriers at those interfaces by alignment of the energy levels is critical for a good device design.

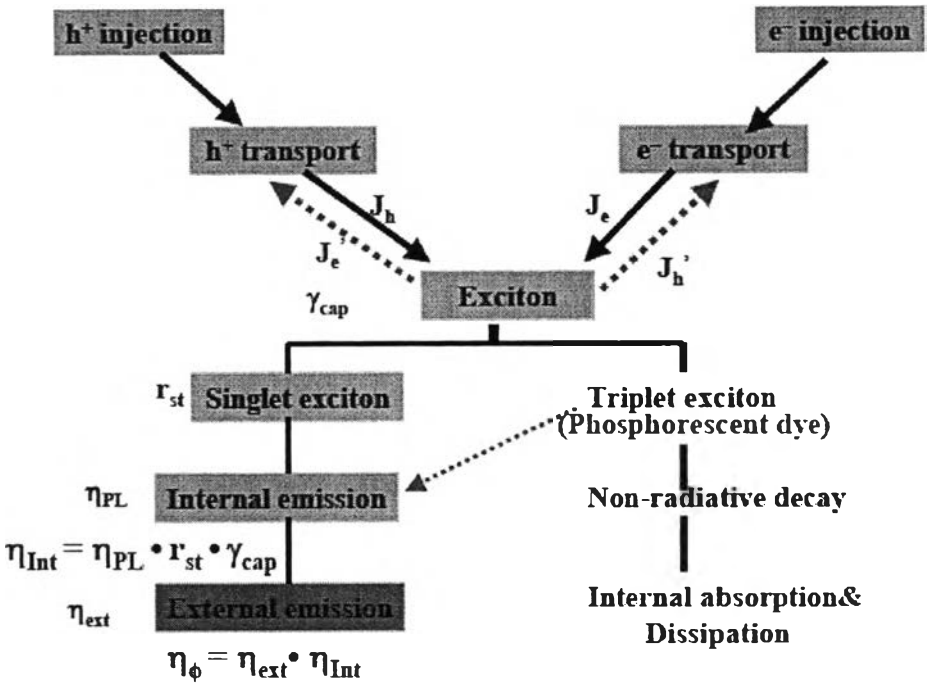

Figure 3.12 OLED working principles, J_h', J_e' stand for leakage current in ETL and HTL respectively. [82]

The external quantum EL efficiency η_φ is defined by the ratio of the number of photons released from the device to the number of charges injected. η_φ can be approximately expressed by $\eta_\varphi = \eta_{ext}\,\eta_{Int}$, where $\eta_{ext} = 1/2n^2$ if based on classical ray optics (n is the refractive index of the emissive medium), internal quantum efficiency η_{Int} is defined by the number of photons produced within a device divided by the number of charge injected. γ_{cap} is the factor of the charge balance, defined by $\gamma = J_r/J$, where J_r is the current used for charge recombination. The meaning of J_r can be explained by Figure 12 based on the mass balance and charge neutrality of hole and electrons. So two equations can be derived as follows: $J=J_h+J_e'=J_e+J_h'$, and $J_r=J_h-J_h'=J_e-J_e'$. If all the holes and electrons are consumed for recombination within an emissive layer, γ_{cap} will be 1.0. If $J_h>>J_e$ or $J_e>>J_h$, γ can be much less than 1.0. Internal quantum EL efficiency can be given by $\eta_{Int} = \gamma_{cap} \cdot r_{st} \cdot \eta_{PL}$, where r_{st} is the

fraction of excitons which are formed as singlets, and η_{PL} is the efficiency of radiative decay of these singlet excitons.

3.2.3 Electron and Hole Injection

Carrier injection is determined by interfacial electronic properties. The understanding of the formation of energy barriers at cathode and anode interfaces is very challenging. The energy barrier at the interfaces is not exactly the difference between the Fermi level of cathode (anode) and the LUMO (HOMO) of the organic layer since there is an ultra-thin dipolar layer at the interface [83]. However, low work function metals such as Mg, Li and Ca can enhance device performance. Electron injection can play a dominant role in the quantum efficiency of OLEDs if there is a large barrier at the ETL/cathode interface.

Carrier injection into a semiconductor can be treated in terms of either Fowler- Nordheim tunneling or Richardson- Schottky (RS) thermionic emission [84]. Both concepts are appropriate in inorganic semiconductors with extended band states and large mean free paths, which is not the case in organic semiconductors. However, Monte Carlo simulation has shown this injection mechanism resembles RS thermionic emission even though quantitative differences exist [85]. The mobility dependence of the thermionic injection rate was first predicted by Emtage and O'Dwyer [86] and extended by Scott and Malliaras [87], introducing the field-dependent factor. The rate of injection at a contact limited electrode is proportional to the charge mobility in the organic material [88]. Specifically, the net injected current into the film is the difference between the injected flux and a surface recombination rate. The injection current can be expressed as the following:

$$J_{INJ} = 4 \Psi^2 N_0 e \mu E \exp(-\varphi_B / kT) \exp(f^{1/2})$$

where Ψ is a slowly varying function of electric field, N_0 is the density of charge hopping sites, and φ_B is the Schottky energy barrier. The exponential in the square

root of the electric field, $f = e^{3} E / [4\pi\varepsilon\varepsilon_0(KT)^2]$, represents the usual Schottky barrier lowering effect.

Recent intensive studies on cathode interface engineering show that electron injection can be enhanced by introducing less than 2 nm ionic compound films such as LiF [89], CaF_2 [21], Li_2O, Cs_2O, NaCl, KCl [90], or by doping the Al cathode in the near interface region with LiF or CsF [91]. The change in image force, determined by the 'f' item in the above formula and caused by inserting the above mentioned high dielectric constant buffer layers, seems to have been overlooked in much of the recent literature. The nature of charge injection is determined by interfacial chemistry that is more complicated than previously assumed [92-94]. Also, it is difficult to quantitatively explain the device electrical characteristics on the basis of injection barrier. The understanding of carrier injection also needs a proper knowledge of transport.

3.2.4 Carrier Transport in Amorphous Organic Semiconductors

OLED materials are conjugated (the bonds between the carbon atoms are alternately single and double). The π electrons are completely delocalized along the conjugated carbons. Hence, their charge transport properties can be affected by the π - π^* molecular orbital overlap. However, the overlap of molecular orbitals for intermolecular electron exchange is much smaller than their inorganic counterparts due to weak van der walls bonding between molecules. Physically, carrier transport in amorphous organic materials depends on the electron-phonon and electron-exchange interactions [95]. It is very challenging to disentangle their intrinsic transport properties directly from the electrical characteristics because of a complicated interfacial situation and unknown trap states. In OLEDs, carrier transport strongly depends on the electric field distribution. There is no universal transport mechanism in a wide temperature range. Phonon assisted thermionic emission might be a dominant mechanism at room temperature (RT). At low temperatures, tunnelling can be dominant for carrier transport between molecules. Carrier transport in OLEDs has been described by space charge limited current

(SCLC) theories at RT if charge injection is not a limiting factor. SCLC obeys the Mott-Gurney equation [96]:

$$JSCLC = (9/8)\,\mu\varepsilon\varepsilon_0\,(V^2/d^3)$$

where μ and ε are mobility and dielectric constant of the material, ε_0 is the permittivity of vacuum, d is the distance between the contacts, and V is the applied voltage.

The space charges can be either free carriers or trapped charges. The early observation of the temperature-dependent power law relation of current-voltage suggested a trapped charge limited current (TCLC) model [97], which employed band models with a distribution of trapping levels below the conduction band. It was developed for bandlike transport rather than hopping transport. Furthermore, constant charge carrier mobility is required, which is contrary to the field-dependence of mobilities [75]. The nature of trapping needs to be clarified for proper device modeling. Thermally stimulated currents (TSC) and thermally stimulated luminescence (TSL) have been used to investigate the trap properties of Alq [98, 99]. The results derived from those spectra are not in good agreement. A trap depth from 0.05 to 0.7 eV and a distribution of trap states from 0.13 to 0.25 eV are suggested by TSC and TSL spectra respectively. TSC spectra vary strongly for Alq of different suppliers [98]. Trap states are more like an extrinsic factor. Very recently, non-dispersive electron transport in well-purified Alq film at nitrogen atmosphere also indicates the trap states might be attributed to impurities and oxygen [100]. Trapping may be seen at very low fields since the free carrier density is lower and may become comparable to the trap concentration. However, at a typical driving voltage of OLEDs, trap-free transport is more like an intrinsic behavior.

The mobility of charge carriers, in amorphous organic materials, is strongly electric field and temperature dependent. Electron transport in amorphous organic films takes place by hopping in the LUMO of each molecule. The energy of LUMO can be assumed to have a Gaussian distribution, with a width of the order of 0.1 eV. A packet of carriers propagating in such a system can quickly reach thermal quasiequilibrium at room temperature [101]. Very limited information about the temperature dependence of OLED material mobility has been provided in the

temperature range from 10 to 70k. In field effect transistors, the mobility in α-sexithiophene (α-6T) displays a nonmonotonic temperature dependence [102]. Above 50 K, the transport is thermally activated, whereas below 40K, the field-effect mobility is approximately temperature independent, as shown in Figure 13.

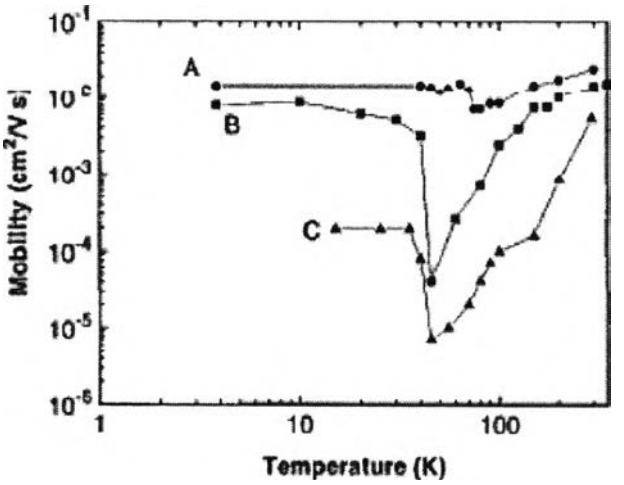

Figure 3.13 Measured μ vs T for three α-6T TFT' A, B and C [102]

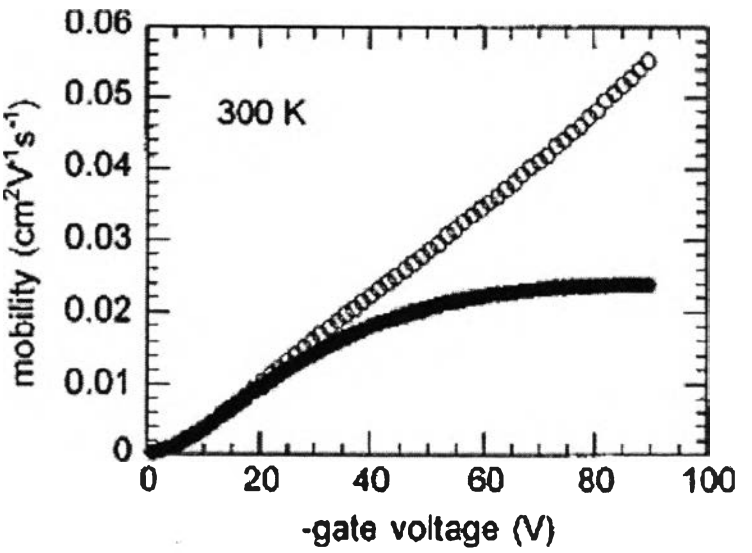

Figure 3.14 Variation of the hole mobility of a 6T poly-crystalline film as a function of gate bias. Data were recorded at 300K. Closed circles correspond to uncorrected data, and open circles to data corrected for the contact series resistance [103].

The hole mobility is also found to increase quasilinearly with gate voltage at room temperature, and that dependence becomes superlinear at low temperatures [103], as shown in Figure 3.14. In silicon field effect transistors, more scattering events can lower the mobility a bit when the carrier density is increased by raising the gate voltage. This abnormal behaviour might indicate some transport coherence in a high carrier density if grain boundaries and defects in thin films are negligible. The picture of charge transport is not very clear. However, a lot of effective experimental work aimed at better electron transport has been done. At driving voltages for a luminance of over 1, 000 cd/m2, usually there is a substantial hole leakage current in ETL, resulting in low current efficiency. N-type doping such as Li [104] can improve the conductivity of ETL and keep a better balance of hole and electron current.

3.2.5 Pairing of Electrons and Holes to Forms Excitons

Spin ½ electron and spin ½ hole can form 4 spin combinations, 3 triplets and 1 singlet. If singlet and triplet capture cross-sections are equal, it implies only 25% efficiency for generation of singlet excitons. This factor is assumed to be insensitive to both devices and materials. Since the ground state of fluorescent molecules is typically singlet, the transition from triplet to singlet is usually forbidden by spin conservation. Thus the maximum internal quantum efficiency is expected to be 25% for fluorescent OLEDs.

Recent studies showed that this is not the case in conjugated polymer [105, 106]. Singlet to triplet ratio depends on the conjugated length [107]. Recombination is spinindependent for the monomer, but that spin-dependent process favoring singlet formation is effective in the polymer as a consequence of the exchange interaction, which will operate on overlapping electron and hole wavefunctions on the same polymer chain at their capture radius [108]. Making use of the triplet excitons can greatly improve quantum efficiency. One approach is to introduce species that will allow efficient triplet luminescence (phosphorescence). This can be provided by high-atomic-number elements with strong spin-orbit coupling. A platinum-

containing porphyrin (PtOEP) has been successfully used as a dopant in molecular OLEDs [109]. The internal quantum efficiency can be as high as 87%.

Under typical working conditions, a potential of order 5V might be applied across a 100 nm thick device. This corresponds to an average applied field of 5×10^7V/m. The local electric field is strongly affected by the presence of space charge and the precise details of the device structure. It may be significantly smaller than this value over therecombination zone. In OLEDs, hopping is the dominant carrier transport mechanism so that the mean free path of charge carriers is roughly the molecular separation. This is about one order of magnitude shorter than the range of the Coulomb interaction. Thus at low fields, recombination can be treated using the carrier motion-controlled Langevin approximation [110]. Nevertheless, at a high-applied field, the size of the carrier capture surface will be greatly reduced. The simple Langevin model is no longer valid. This behaviour can be explained by the Thomson-like recombination controlled by the carrier capture [111].

3.2.6 Photon Released out from OLED

The coupling of electronic excitations to photon states is affected by the physical structure of OLEDs. The presence of the metallic cathode provides a mirror that modifies the pattern of the electromagnetic modes near the cathode. The variation of Alq film thickness in a two-layer structure will change the distance between the emissive zone and the cathode, therefore emission spectra, as shown in Figure 3.15, and spectral emission patterns will change accordingly. The emission pattern could deviate from the ideal Lambertian pattern [112]. This dependence of emission pattern on Alq thickness cannot be explained by classical optics.

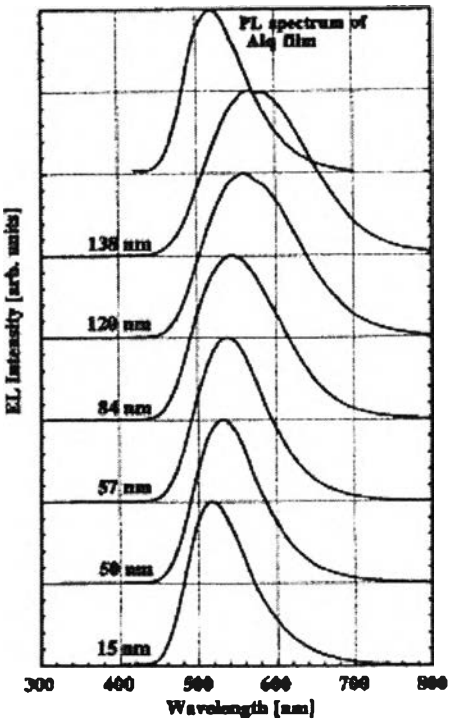

Figure 3.15 Electroluminescence spectra at normal directions in ITO/TPD (50 nm)/Alq/MgAg devices [112]

Due to the refractive index mismatch between the emitting layer and air, a large fraction of the light is trapped in the glass, ITO, and organic layers. The external coupling efficiency is estimated by classical theory to be $1/2n_2$ for large n [113]. The external coupling efficiency in planar organic light-emitting devices can be modeled based on a quantum mechanical microcavity theory [114] and measured by examining both the far field emission pattern and the edge emission of light trapped in the glass substrate. The external coupling efficiency is dependent upon the thickness of the ITO layer and the refractive index of the substrate. The coupling efficiency ranges from 24% to 52%, but in general it is much larger than the 18.9% expected from classical ray optics [115]. It is clear that the results obtained from ray optics can overestimate the internal quantum efficiency.

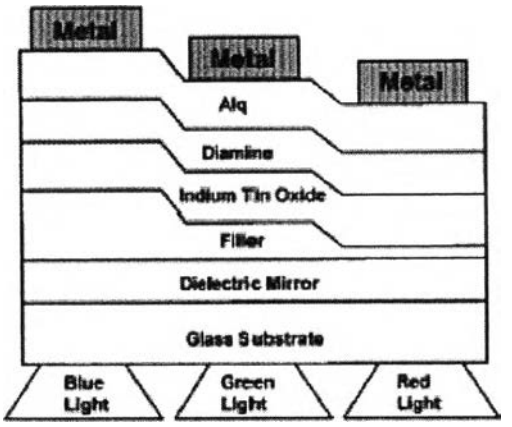

Figure 3.16 Schematic layer structure of a patterned planar microcavity in which the Si_3N_4 filler layer is etched to three different thicknesses to change the optical properties [116]

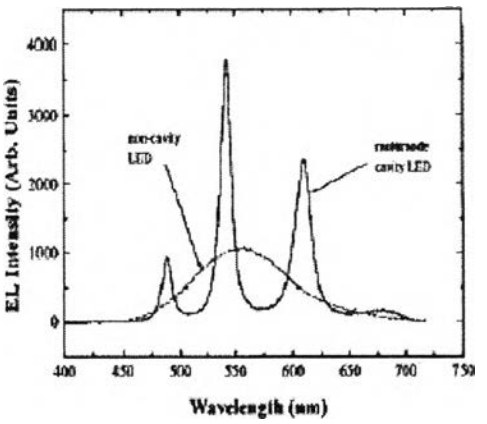

Figure 3.17 Electroluminescence spectrums from a three-mode microcavity LED, in which the three peaks are at 488, 543, and 610 nm [116]

After adding a multilayer dielectric stack on the other side of the ITO from the organic layer, this stack, along with the metal cathode, forms a resonant cavity with a narrow band pass that can be selected by varying the optical thickness of the cavity [116, 117]. With an emitting layer that has a white spectrum, the three primary colors can be obtained by patterning different dielectric thicknesses as indicated in Figures 3.16 and 3.17. This technology is promising for RGB colors even though close control of the etching process is required.

Here, the detail presented above is the fundamental theory of organic light emitting diodes (OLEDs). Up to the present time, the novel concept of OLEDs is to develop by printed electronic in order to obtain the flexible display.

3.3 Flexible Substrate for Organic Light Emitting Diodes (OLEDs)

Flexible substrate for organic light emitting diodes (OLEDs) has been successfully developed up to the present time in order to replace the use of flat substrate. The flexible display can be classified according to degree of flexibility. Flat displays are made of plastic or another non-glass backplane, but only for the benefit of lightness or ruggedness; formed displays are bent once, such as a curved automobile dashboard, but do not flex further. However, flexible displays can be bent or flexed during use. The definition of flexible displays can be extent to the rollable process of flexible display fabrication.

The prospects for flexible displays are promising, although the timing still depends on technical and manufacturing developments [118, 119]. Electrophoretic displays such as electronic papers using plastic substrates, which have a relatively simple structure, are just beginning to be produced in quantities approaching high volume. Displays that are intended to flex or roll during use may reach the market in several years, pending further developments in backplane and fabrication processes. The near-term revenue in dynamic signage and mobile phones will lead to the development of larger and more sophisticated displays with flexibility and rollability. Figure 3.18, which has been adapted from the data of the iSuppli Flexible Display Report, shows the market prospects for flexible displays from 2007 to 2013 [120].

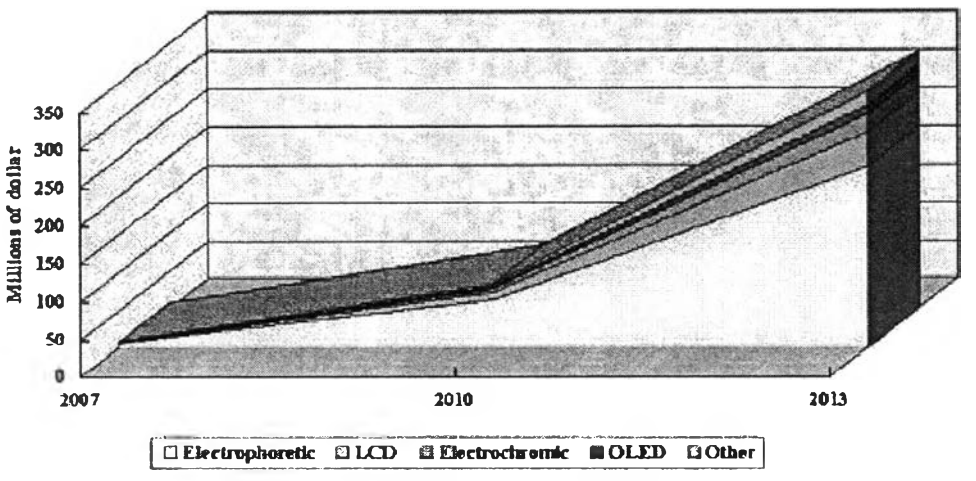

Figure 3.18 Market prospect for flexible displays [8]

Polymers are very promising materials for flexible displays with many advantages. They are transparent, light in weight, flexible, and robust. Polymers are a good alternative to the glass substrates that have been actively used for flat panel displays such as liquid crystal displays (LCDs) and plasma discharge panels (PDPs). Glass is so rigid that it is very difficult to use in a flexible display. Polymers have mechanical properties that vary from strong rigidity, such as in engineering plastics, to softness, such as in rubber or polyethylene films. They are some of the least expensive materials and are suitable for mass production via roll-to-roll (RTR) processes. Therefore, polymers are being considered as the key materials for flexible displays in various application areas including transparent substrates, electrodes, active materials for organic light emitting devices (OLEDs), LCDs and organic thin-film transistors (OTFTs), dielectric materials, and coating materials. All polymer-based flexible displays are being investigated.

3.3.1 Potential Polymer Candidate For Flexible Display

There are several polymers that are candidates for flexible substrates as shown in Figure 3.19, which lists substrates in terms of glass transition emperature (Tg) [121].

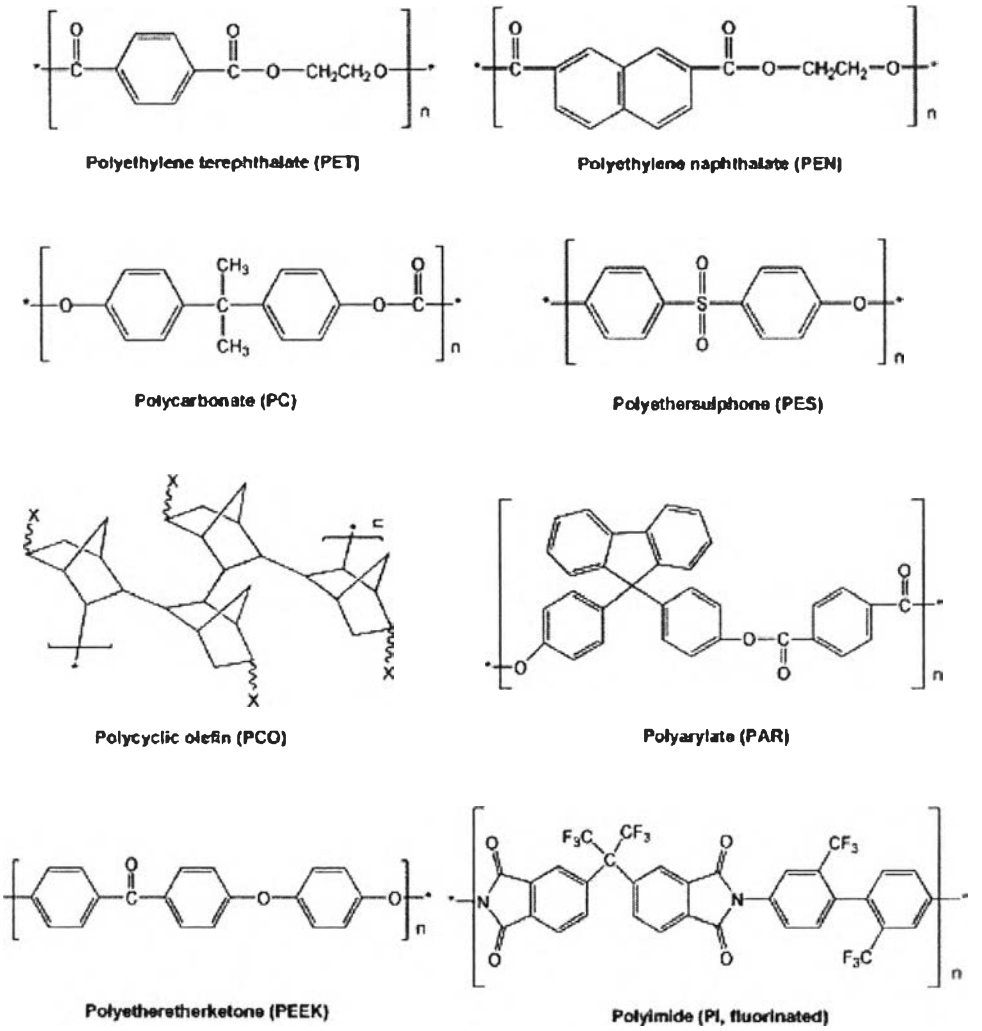

Figure 3.19 Potential candidate polymers for flexible display substrate

These polymers are divided into three types, including crystalline, amorphous, and solution-castable amorphous. Thermoplastic semi-crystalline polymers available for flexible displays include polyethylene terephthalate (PET), polyethylene naphthalate (PEN), and polyetheretherketone (PEEK) [122, 123]. PEEK, whose Tg and Tm are 140 and 340 °C, respectively, is known be at the upper limit of semicrystalline polymers that can be melt-processed because polymers with a Tg of higher than 140 °C will be degraded significantly during a melt process. Heat-stabilized semi-crystalline polymers provide good dimensional stability above their Tg, which expands their upper operating temperature. The second group, amorphous polymers, includes polycarbonate (PC) and polyethersulphone (PES) [124]. These are non-crystalline thermoplastics that can be melt-extruded or solvent casted. The

last group is the amorphous polymers that cannot be melt-processed, such as modified PC, polyacrylate (PAR), polycyclic olefin (PCO) or polynorbonene (PNB), and polyimide (PI) [125-127]. Fabric materials [128], ultra-thin polymer films [129], and glass reinforced plastic [130] have also been used as substrates. Figure 3.20 summarizes the Tg of the candidate polymers for flexible substrates.

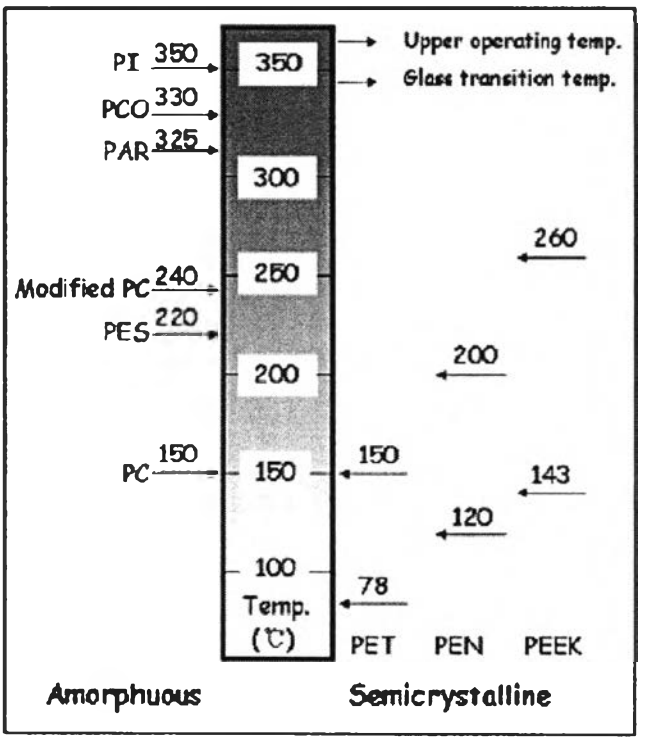

Figure 3.20 Glass transition temperature (Tg) of commercially available polymer

3.3.2 Properties Requirement of Polymer for Flexible Display Substrate

The properties requirement of flexible display devices are currently based on glass substrate because they are perfectly satisfactory for flat panel display applications. In order to replace glass, a polymer substrate needs to have the general properties same as glass including clarity, dimensional stability, thermal stability, barrier properties, solvent resistance, smooth surface as well as excellence in optical properties.

Clarity

Clarity is the most important property for bottom emissive displays, and a total light transmission of > 85% over 400-800 nm coupled with a haze of less than 0.7% are typical of what is required [121].

- Thermal stability

Thermal stability is another issue for polymer substrates. Polymer substrates are exposed to high temperatures during manufacturing processes such as barrier coating [131], electrode deposition [132] and patterning [133].

There are two factors that have to be considered when selecting polymer materials with the proper thermal stability: CTE and Tg, where polymer chains start to move for stress relaxation that is stored during the processes. In general inorganic or metal layers used for barrier or electrode layers have much lower CTE than polymer substrates, and the dimensions of the polymer change significantly at Tg. Polymer with high Tg are better alternative candidate for this regard. However, in order to maintain the flexibility aspect of substrate, Tg at room temperature of polymer is considered. The important point of this issue is to select appropriate polymer for flexibility and high temperature resistance optimization.

On the other hand, a low CTE is also advantageous for making dimensionally stable designs for devices [125]. A mismatch of CTE between layers gives rise to strain and cracking under thermal cycling during device fabrication.

Therefore, the Tg at room temperature and CTE lower than 20 ppm K^{-1} are required for flexible substrate of OLEDs fabrication [121].

- Surface properties

Surface qualities such as roughness and cleanliness are essential to ensure the integrity of subsequent layers including barrier and conductive layers. Semi-crystalline polymer films do not possess good surface properties compared to amorphous polymer films. Surface defects that remain in the substrates are detrimental to the performance of the active layer of OLEDs. They will creat defects like pinholes on the thin films of barrier and electrodes, forming dark spots in OLEDs [134]. The defects will also lead to cracks when display is bent. However, to

provide a defect-free surface, scratch resistant or planarizing layers are coated to smooth over entire underlying substrate surface [135]. The coated film ensures good integrity for subsequent barrier layers and conductive coating.

Therefore, in case of flat substrate, the smoothness of surface should be preferably less than 10 nm [8].

- Chemical resistance

Polymer substrates have to be exposed to a wide range of solvents as well as moisture during manufacturing processes, including cleaning, coating and patterning process. Normally, there is a typical list of the materials that the substrate must be compatible with includes methanol, isopropanol, acetone, THF, etc. Coated polymer substrates with a variety of organic or inorganic layers or a hard coating layer are used to prevent the invasion of solvents and moisture [121].

- Mechanical properties

For the roll to roll (RTR) process as well as display performance, mechanical properties have to be carefully considered [136]. Flexible OLEDs which demand stringent requirements among the display technologies, usually contain a polymer substrate, organic-inorganic multi barrier layer and encapsulation layers are exhibited in Figure 3.21.

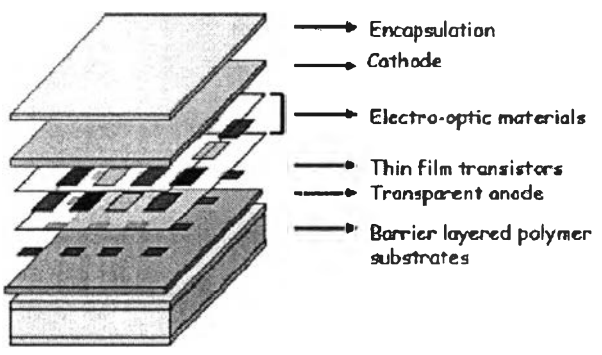

Figure 3.21 Cross-sectional structure of flexible displays

When the devices are bent, the mechanical discrepancy at the interface between the organic and inorganic materials generates mechanical failure in devices. Foe these device with inorganic thin films may be a source of failure due to their

brittle properties [137]. Therefore, organic thin film is preferably used for rollable displays.

However, the failure of devices depends on the arrangement, thickness and properties of all layers. Adhesion at the interfaces between the different layers under thermal cycling and environmental testing, wetting characteristics and the ability to withstand flex testing are critical to determine their robustness during use [138].

- Water vapor transmission rate (WVTR) and Oxygen transmission rate (OTR)

Normally, polymer substrates are sensitive to moisture and air. The electronic devices, especially OLEDs demand more stringent barrier confinement. For an OLED lifetime of > 10000h, the requirements include water vapor transmission rates (WVTR) of 10^{-6} g/m^2/day and OTR of 10^{-5} mL/m^2/day [139, 140]. Figure 3.22 shows the relative barrier properties and requirements for electro-optic devices.

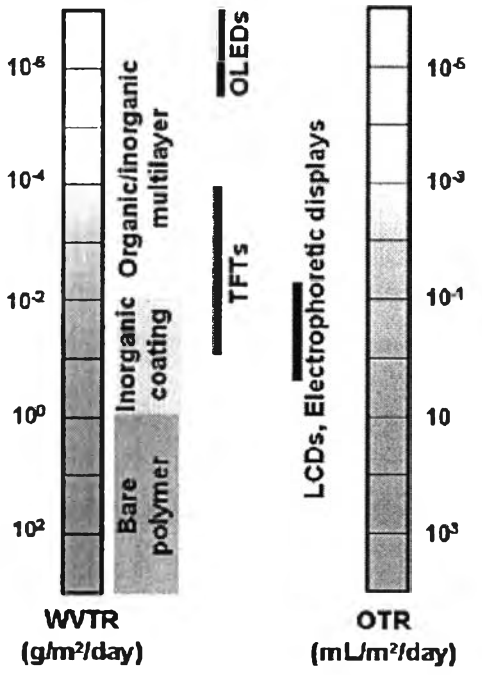

Figure 3.22 Requirement of WVTR and OTR for electronic devices [8]

In order to prevent this issue, inorganic transparent thin film has been widely used as barrier layer. Silicon and aluminum oxide can be deposited on polymer substrate by plasma enhanced chemical vapor deposition (PECVD) [141], sputtering or evaporation.